

The Role of Confined Water in Ionic Liquid Electrolytes for Dye Sensitized Solar Cells

Jiwon Jeon^{a,‡}, Hyungjun Kim^{a,‡,}, William A. Goddard III^{a,b,d,*}, Tod A.
Pascal^{a,b}, Ga-In Lee^c, and Jeung-Ku Kang^{a,c}*

^aGraduate School of Energy Environment Water Sustainability (EEWS), Korea Advanced Institute of Science and Technology, Daejeon, 305-701, Republic of Korea

^bMaterials and Process Simulation Center, Beckman Institute, California Institute of Technology, Pasadena, CA 91125

^cMaterials Science, Korea Advanced Institute of Science and Technology, Daejeon, 305-701, Republic of Korea

^dWorld Class University (WCU) Professor in the EEWS/KAIST

[‡]These authors contributed equally.

*To whom correspondence should be addressed:

E-mail: H.K. (linus16@kaist.ac.kr) and W.A.G. (wag@wag.caltech.edu)

S.1 Simulation Details To achieve an equilibrium description of ionic liquid (IL) systems, we carried out molecular dynamics (MD) simulations using the cohesive energy density (CED) formalism¹; as follows:

- 1) we used the Monte Carlo procedure in the Amorphous builder module of Cerius2 (Accelrys, San Diego) to construct initial structures with an expanded unit cell chosen to lead to half the experimental density² of 1.5 g/cm³:
- 2) we carried out 15 to 20 cycles of annealing dynamics, where each cycle consists of heating at a uniform rate from 300K-to-600K and then cooling from 600K-to-300K over a total of 0.2 ns and chose the structure with the most negative potential energy from the trajectory of the annealing dynamics for the next step
- 3) we compressed the unit cell by a factor of 2.2 until a density of 1.65 g/cm³ was reached, (1.1 times higher than the experimental density
- 4) At the final density of 1.65 g/cm³ we carried out NVT MD (constant volume with a Nosé-Hoover thermostat using a 0.1 ps damping constant) at 300K for 1 ns;
- 5) Finally we performed 2 ns NPT MD (Nosé-Hoover thermostat and Andersen barostat with 1 ps damping constant) at 300K and 1 atm leading to an equilibrium density of 1.63 g/cm³ for 0 % water;
- 6) Finally at the final density from step 6, we performed 30 ns of NVT MD, using the last 10 ns for analyses of properties.

S.2 Amount of Absorbed Water into IL at Vapor-IL Equilibrium The chemical potential ($\mu = \partial A / \partial n_{\text{WAT}}$) of water in gas and IL has the form

$$\mu_{\text{WAT}(g)} = \mu_{\text{WAT}(g)}^{\circ} + RT \ln(P^{\text{SAT}}) \quad (\text{S1})$$

$$\mu_{\text{WAT}(IL)} = \mu_{\text{WAT}(IL)}^{\circ} + RT \ln(P_{\text{WAT}(IL)}) \quad (\text{S2})$$

where the superscript $^{\circ}$ indicates the standard state ($T=300\text{K}$, $P=1\text{atm}$), R is the molar gas constant ($8.314 \text{ J mol}^{-1} \text{ K}^{-1}$), T is 300K , and P^{SAT} is the saturated vapor pressure of water (0.031 atm at 25°C).

Assuming $P_{\text{WAT}(IL)} = \chi_{\text{WAT}(IL)}$, reduces Eq. S2 to

$$\mu_{\text{WAT}(IL)} = \mu_{\text{WAT}(IL)}^{\circ} + RT \ln(\chi_{\text{WAT}(IL)}) \quad (\text{S3})$$

At vapor-IL equilibrium, the chemical potential of the water is identical, $\mu_{\text{WAT}(g)} = \mu_{\text{WAT}(IL)}$, leading

$$\chi_{\text{WAT}(IL)} = \exp[\mu_{\text{WAT}(g)}^{\circ} - \mu_{\text{WAT}(IL)}^{\circ} / RT] P^{\text{SAT}} \quad (\text{S4})$$

Under ambient condition having 60~70% humidity, Eq. S4 yields the equilibrium amount of absorbed water in IL as $\chi_{\text{WAT}} = 9 - 10.5 \%$, which supports for the experimental observances from titration and IR measurements³.

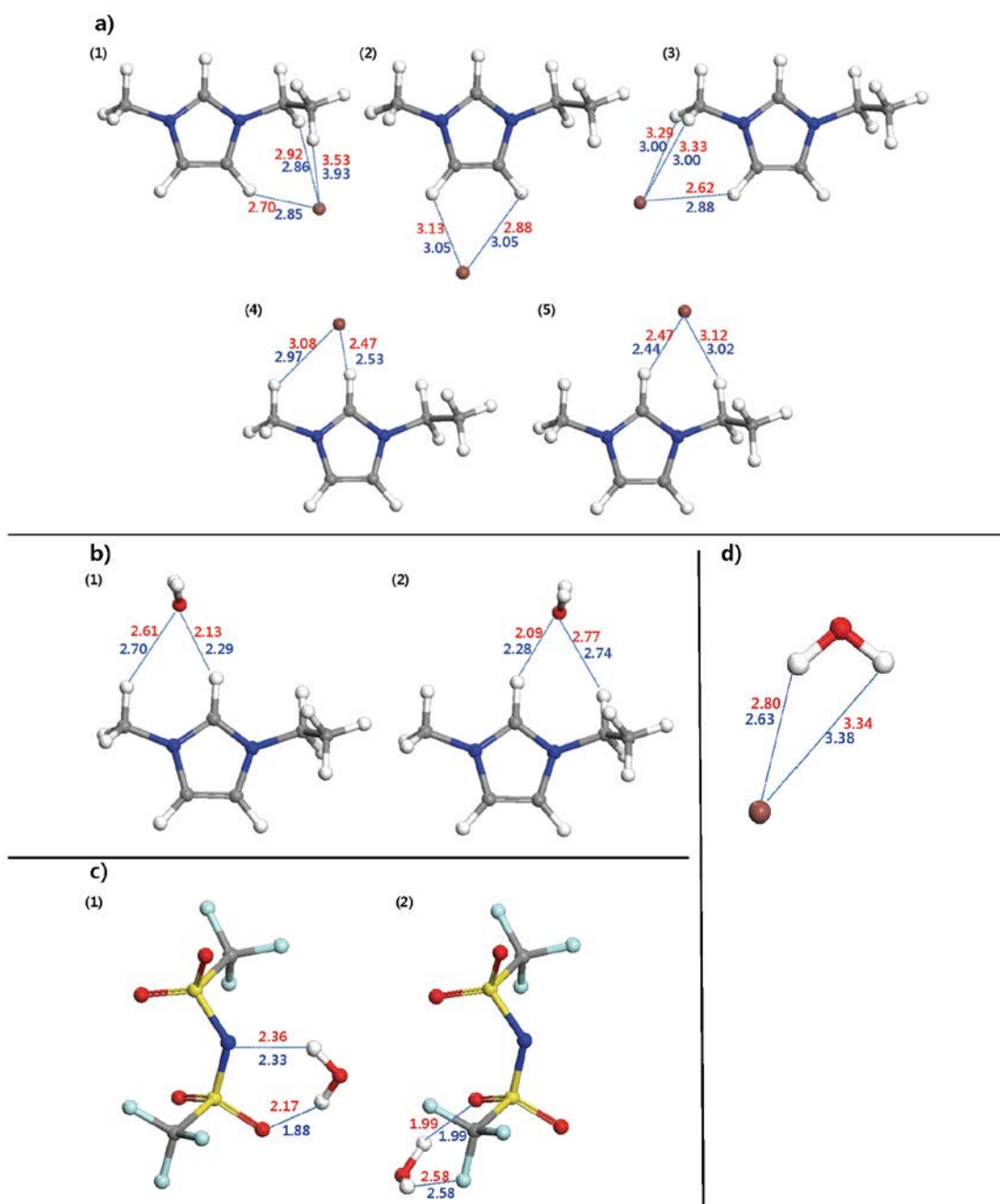


Fig. S1 The final structure from QM (quantum mechanics) in red and FF (force field) calculations in blue.
a) Stable structures of I⁻ around EMIm⁺.
b) Stable structures for water interacting with EMIm⁺.
c) Stable structures for water interacting with TFSI.
d) Stable structures for water interacting with I⁻.
 These comparisons show that the optimized FF parameters lead to structures in good agreement with QM.

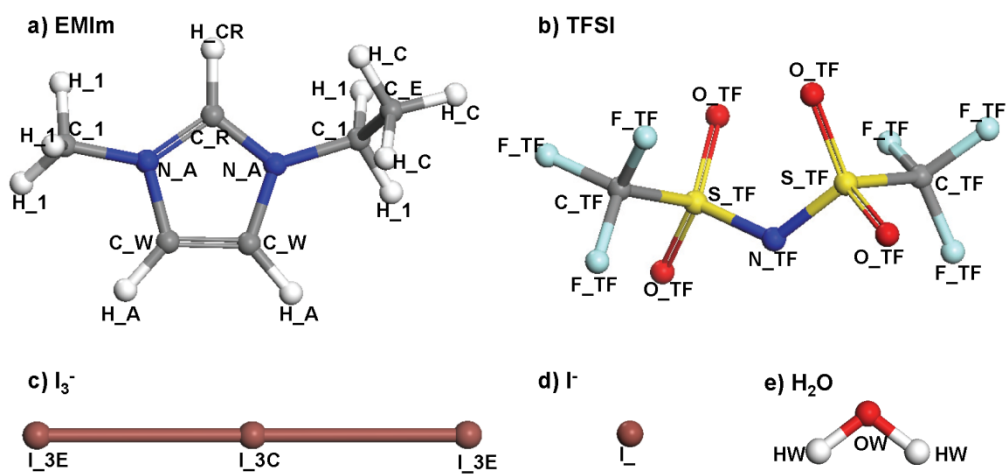


Fig. S2 Atom types for our first-principle based Force-fields.

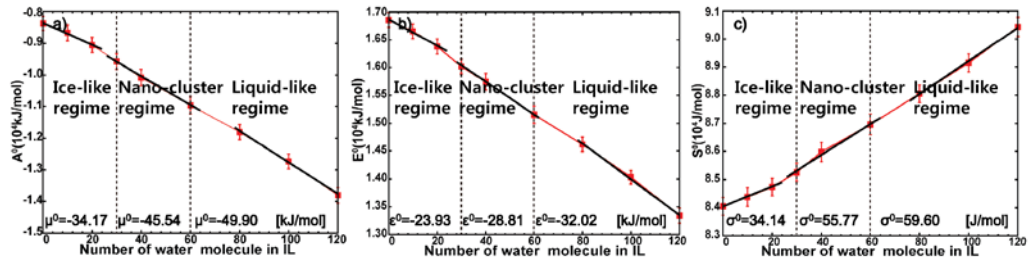


Fig. S3 a) The Helmholtz free energy (A) as a function of water content. μ^0 stands for $\partial A^0 / \partial n_{WAT}$. b) internal energy as function of water content. ε^0 stands for $\partial E^0 / \partial n_{WAT}$. c) entropy as function of water content. The σ^0 stands for $\partial S^0 / \partial n_{WAT}$. This shows that the molecular state of water depends on the water concentration in IL.

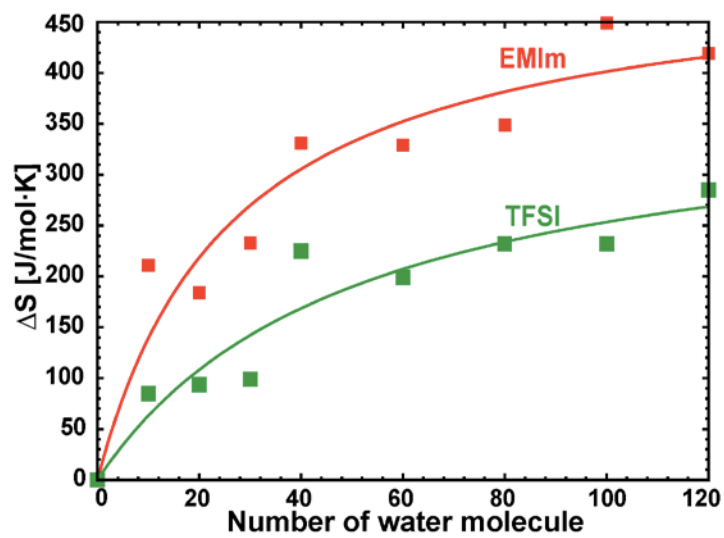


Fig. S4 The entropy of EMIm (red) and TFSI (green) is enhanced with increased water content in IL, leading to increase total entropy.

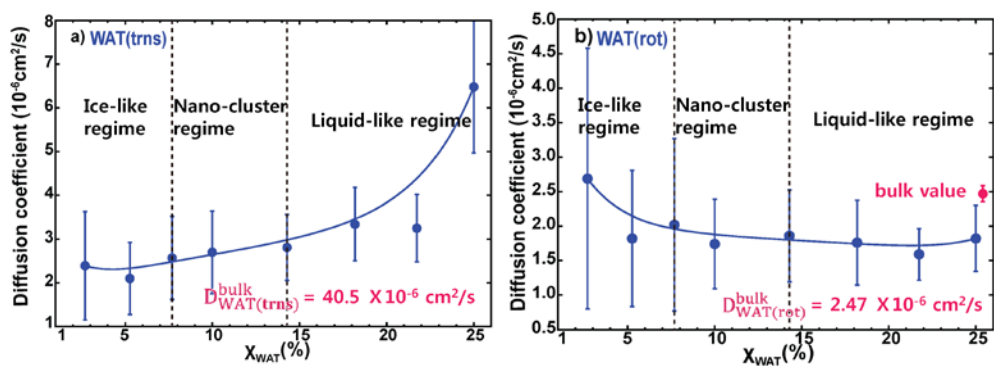


Fig. S5 a) The translational contribution to the diffusivity of water. , b) The rotational contribution to the diffusivity of water Since water in IL has hydrogen bonding with ions the rotational diffusivity of water molecule is decreased

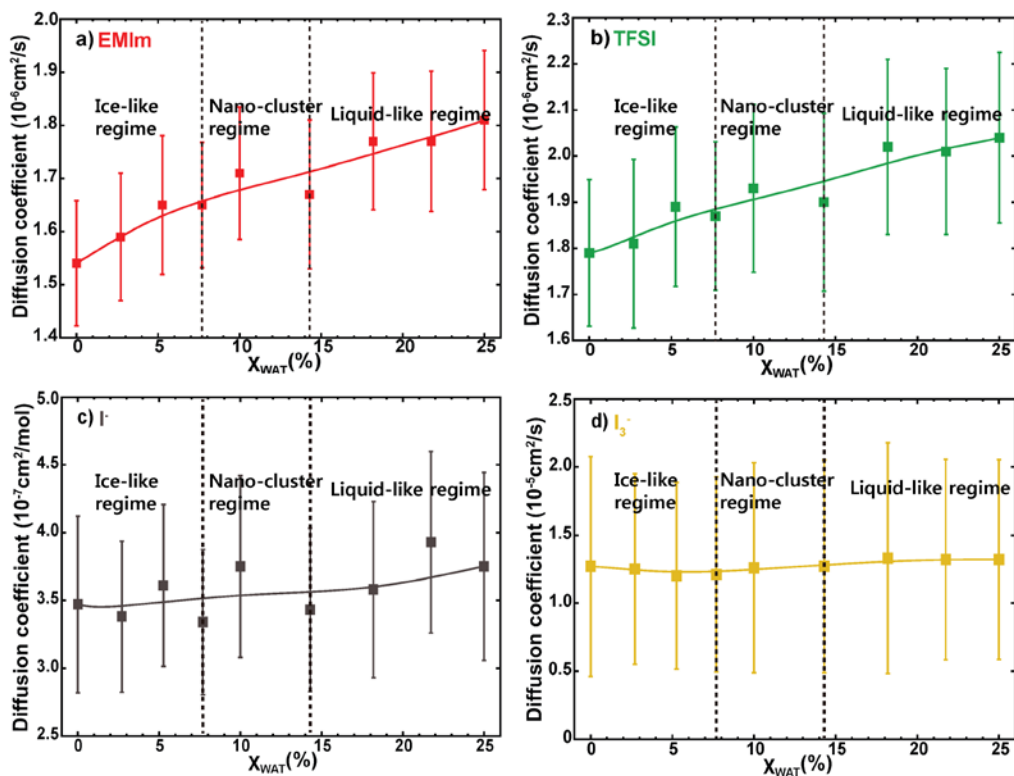


Fig. S6 Green-Kubo Diffusivity of **a)** EMIm⁺ and **b)** TFSI as a function of water content. Both increase significantly particularly in the *ice-like* regime (0-5.26 mole fraction of water). **c)** The diffusivity of I⁻ and **d)** I₃⁻ as a function of water content.

Table S1 Comparison of the binding energy between QM and FF calculation for various structures.

- a) For EMIm⁺ and I⁻, the error is less than ~1 kcal/mol for the optimal binding sites (4 and 5).
- 2) For EMIm⁺ and water, the difference of binding energy between QM and FF is within 0.2 kcal/mol.
- 3) For TFSI⁻ and water, the difference of binding energy between QM and FF is within ~2.3 kcal/mol.
- 4) For I⁻ and water, the difference of binding energy between QM and FF is 0.36 kcal/mol.

		EMIm-I ⁻					EMIm-WAT		TFSI-WAT		I-WAT
Position		1	2	3	4	5	1	2	1	2	1
Binding Energy [kcal/mol]	QM	73.51	70.15	76.07	81.68	81.97	10.00	9.92	9.04	10.83	12.56
	FF	70.20	66.53	73.51	81.64	80.92	9.83	9.99	7.09	8.54	12.20
	Differ	3.31	3.62	2.56	0.04	1.05	0.17	0.07	1.95	2.29	0.36

Table S2 Optimized Force field parameters for ionic liquid systems with water, iodide, and tri-iodide. See Fig. S2. VdW interactions are described with 12-6 Lennard-Jones potential, $U(r) = D_0 \left(\left(\frac{R_0}{r} \right)^{12} - 2 \left(\frac{R_0}{r} \right)^6 \right)$.

VdW on Diagonal term		$R_0(\text{Å})$	$D_0(\text{kcal/mol})$
I_		4.8246	0.2215
I_3E		4.8246	0.2215
I_3C		4.8246	0.2215
VdW off Diagonal term		$R_0(\text{Å})$	$D_0(\text{kcal/mol})$
I_	H_CR	2.8640	0.5000
I_	H_1	3.1000	1.4000
OW	H_CR	2.9177	0.0553
OW	I_	4.1550	0.4000

- (1) Belmares, M.; Blanco, M.; Goddard, W. A.; Ross, R. B.; Caldwell, G.; Chou, S. H.; Pham, J.; Olofson, P. M.; Thomas, C. *Journal of Computational Chemistry* **2004**, *25*, 1814.
- (2) Noda, A.; Hayamizu, K.; Watanabe, M. *Journal of Physical Chemistry B* **2001**, *105*, 4603.
- (3) Cammarata, L.; Kazarian, S. G.; Salter, P. A.; Welton, T. *Phys. Chem. Chem. Phys.* **2001**, *3*, 5192.